

Article

Robust Representation and Efficient Feature Selection Allows for Effective Clustering of SARS-CoV-2 Variants

Zahra Tayebi ¹, Sarwan Ali ² and Murray Patterson ^{3,*}

¹ Georgia State University, Atlanta, GA, USA; ztayebi1@student.gsu.edu

² Georgia State University, Atlanta, GA, USA; sali85@student.gsu.edu

³ Georgia State University, Atlanta, GA, USA; mpatterson30@gsu.edu

* Correspondence: mpatterson30@gsu.edu

Version October 20, 2021 submitted to Journal Not Specified

Abstract: The widespread availability of large amounts of genomic data on the SARS-CoV-2 virus, as a result of the COVID-19 pandemic, has created an opportunity for researchers to analyze the disease at a level of detail unlike any virus before it. One one had, this will help biologists, policy makers and other authorities to make timely and appropriate decisions to control the spread of the coronavirus. On the other hand, such studies will help to more effectively deal with any possible future pandemic. Since the SARS-CoV-2 virus contains different variants, each of them having different mutations, performing any analysis on such data becomes a difficult task. It is well known that much of the variation in the SARS-CoV-2 genome happens disproportionately in the spike region of the genome sequence — the relatively short region which codes for the spike protein(s). Hence, in this paper, we propose an approach to cluster spike protein sequences in order to study the behavior of different known variants that are increasing at very high rate throughout the world. We use a k-mers based approach to first generate a fixed-length feature vector representation for the spike sequences. We then show that with the appropriate feature selection, we can efficiently and effectively cluster the spike sequences based on the different variants. Using a publicly available set of SARS-CoV-2 spike sequences, we perform clustering of these sequences using both hard and soft clustering methods and show that with our feature selection methods, we can achieve higher F1 scores for the clusters.

Keywords: COVID-19; SARS-CoV-2; Spike Protein Sequences; Cluster Analysis; Feature Selection; k-mers

1. Introduction

The virus that causes the COVID-19 disease is called the severe acute respiratory syndrome coronavirus 2 (SARS-CoV-2) — a virus whose genomic sequence is being replicated and dispersed across the globe at an extraordinary rate. The genomic sequences of a virus can be helpful to investigate outbreak dynamics such as spatiotemporal spread, the size variations of the epidemic over time, and transmission routes. Furthermore, genomic sequences can help design investigative analyses, drugs and vaccines, and monitor whether theoretical changes in their effectiveness over time might refer to changes in the viral genome. Analysis of SARS-CoV-2 genomes can therefore complement, enhance and support strategies to reduce the burden of COVID-19 [1].

SARS-CoV-2 is a single-stranded RNA-enveloped virus [2]. Its entire genome is characterized by applying an RNA-based metagenomic next-generation sequencing method. The length of the genome is 29,881 bp (GenBank no. MN908947), encoding 9860 amino acids [3]. Structural and nonstructural proteins



Figure 1. The SARS-CoV-2 genome is roughly 29–30kb in length, encoding structural and non-structural proteins. Open reading frame (ORF) 1ab encodes the non-structural proteins, and the four structural proteins: S (spike), E (envelope), M (membrane), and N (nucleocapsid) are encoded by their respective genes. The spike protein has 1274 amino acids.

are expressing the gene fragments. Structural proteins are encoded by the S, E, M and N genes, while the ORF region encodes nonstructural proteins [4] (see Figure 1).

A key factor involved in infection is the S protein on the surface of the virus [5]. The S protein of SARS-CoV-2 is similar to other coronaviruses and arbitrates receptor recognition, fusion, and cell attachment through viral infection [6–8]. The S protein has an essential role in viral infection that makes it a potential target for vaccine development, antibody-blocking therapy, and small molecule inhibitors [9]. Also, the spike region of the SARS-CoV-2 genome is involved in a disproportionate amount of the genomic variation, for its length [10] (see, *e.g.*, Table 1). Therefore, mutations that affect the antigenicity of the S protein are of certain importance [11].

Generally, the genetic variations of a virus are grouped into clades, which can also be called subtypes, genotypes, or groups. To study the evolutionary dynamics of viruses, building phylogenetic trees out of sequences is common [12]. On the other hand, the number of available SARS-CoV-2 sequences is huge and still increasing [13] — building trees on the millions of SARS-CoV-2 sequences would be very expensive and seems impractical. In these cases, machine learning approaches that have flexibility and scalability could be useful [14]. Since natural clusters of the sequences are formed by the major clades, clustering methods would be useful to understand the complexity behind the spread of the COVID-19 in terms of its variation. Also by considering the certain importance of the S protein, we focus on the amino acid (protein) sequences encoded by the spike region. In this way, we would reduce the dimensionality of data without losing too much information, reducing the time and storage space required and making visualization of the data easier [15].

To make use of machine learning approaches, we need to prepare the appropriate input — numerical (real-valued) vectors — that is compatible with these methods. This would give us the ability to perform meaningful analytics. As a result, these amino acid sequences should be converted into numeric characters in a way that preserves some sequential order information of the amino acids within each sequence. The most prevalent strategy in this area is one-hot encoding due to its simplicity [10]. Since we need to compute pairwise distances (*e.g.*, Euclidean distance), one-hot encoding order preservation would not be operational [16]. To preserve order information of each sequence while being amenable to pairwise distance computation, k -mers (length k substrings of each sequence) are calculated and input to the downstream classification/clustering tasks [16,17] (see Figure 2).

The proposed methods in this study are fast and efficient clustering methods to cluster the spike amino acid sequences of SARS-CoV-2. We demonstrate that our method performs considerably better than the basic methods, and the variants are successfully clustered into unique clusters with high F_1 score. The following are the contributions of this paper:

1. For efficient sequence clustering, we propose a method based on k -mers, and show that the downstream clustering methods successfully cluster the variants with high F_1 score.
2. We performed experiments using different clustering algorithms and feature selection approaches and show the trade-off between the clustering quality and the runtime for these methods.

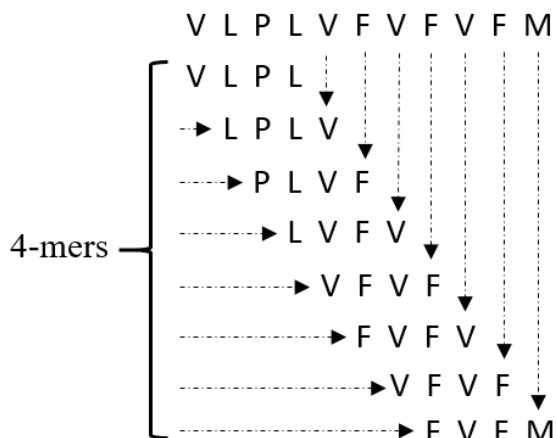


Figure 2. Example of 4-mers of the amino acid sequence “VLPLV F V F V F M”.

3. We use both hard and soft clustering approaches to study the behavior of different coronavirus variants in detail.

The rest of the paper is organized as follows: Section 2 contains related work of our approach. Our proposed approach is detailed in Section 3. A description of the datasets used are given in Section 4. We provide a detailed discussion about the results in Section 5, and then we conclude our paper in Section 6.

2. Literature Review

Performing different data analytics tasks on sequences has been done successfully by different researchers previously [16,18]. However, most studies require the sequences to be aligned [10,19,20]. The aligned sequences are used to generate fixed length numerical embeddings, which can then used for tasks such as classification and clustering [16,21,22]. Since the dimensionality of data is another problem while dealing with larger sized sequences, using approximate methods to compute the similarity between two sequences is a popular approach [17,23,24]. The fixed-length numerical embedding methods have been successfully used in literature for other applications such as predicting missing values in graphs [25], text analytics [26–28], biology [17,23,29], graph analytics [30,31], classification of electroencephalography and electromyography sequences [32,33], detecting security attacks in networks [34], and electricity consumption in smart grids [35,36]. The conditional dependencies between variables is also important to study so that their importance can be analyzed in detail [37].

Due to the availability of large-scale sequence data for the SARS-CoV-2 virus, an accurate and effective clustering method is needed to further analyze this disease, so as to better understand the dynamics and diversity of this virus. To classify different coronavirus hosts, authors in [10] suggest a one-hot encoding-based method that uses spike sequences alone. Their study reveals that they achieved excellent prediction accuracy considering just the spike portion of the genome sequence instead of using the entire sequence. Using this idea and a kernel method, Ali et al., in [16] accomplish higher accuracy than in [10], in classification of different variants of SARS-CoV-2 in humans. Successfully analysis of different variants leads to designing efficient strategy regarding the vaccination distribution [38–41].

3. Proposed Approach

In this section, we discuss our proposed algorithm in detail. We start with the description of k -mers generation from the spike sequences. We then describe how we generated the feature vector representation

from the k -mers information. After that, we discuss different feature selection methods in detail. Finally, we detail how we applied clustering approaches on the final feature vector representation.

3.1. k -mers Generation

Given a spike sequence, the first step is to compute all possible k -mers. The total number of k -mers that we can generate for a spike sequence are described as follows:

$$N - k + 1 \quad (1)$$

where N is the length of the spike sequence ($N = 1274$ for our dataset). The variable k is a user-defined parameter (we took $k = 3$ using standard validation set approach [42]). For an example of how to generate k -mers, see Figure 2.

3.2. Fixed-Length Feature Vector Generation

Since most of the Machine Learning (ML) models work with a fixed-length feature vector representation, we need to convert the k -mers information into the vectors. For this purpose, we generate a feature vector Φ_k for a given spike sequence a (*i.e.*, $\Phi_k(a)$). Given an alphabet Σ (characters representing amino acids in the spike sequence), the length of $\Phi_k(a)$ will be equal to the number of possible k -mers of a . More formally,

$$\Phi_k(a) = |\Sigma|^k \quad (2)$$

Since we have 21 unique characters in Σ (namely $ACDEFGHIKLMNPQRSTVWXY$), the length of each frequency vector is $21^3 = 9261$.

3.3. Low Dimensional Representation

Since the dimensionality of data is high after getting the fixed length feature vector representation, we apply different supervised and unsupervised methods to obtain a low dimensional representation of data to avoid the problem of the *curse of dimensionality* [35,43]. Each of the methods for obtaining a low dimensional representation of data is discussed below:

3.3.1. Random Fourier Features

The first method that we use is an approximate kernel method called Random Fourier Features (RFF) [44]. It is an unsupervised approach, which maps the input data to a randomized low dimensional feature space (euclidean inner product space) to get an approximate representation of data in lower dimensions D from the original dimensions d . More formally:

$$z : \mathcal{R}^d \rightarrow \mathcal{R}^D \quad (3)$$

In this way, we approximate the inner product between a pair of transformed points. More formally:

$$f(x, y) = \langle \phi(x), \phi(y) \rangle \approx z(x)'z(y) \quad (4)$$

In Equation (4), z is low dimensional (unlike the lifting ϕ). Now, z acts as the approximate low dimensional embedding for the original data. We can use z as an input for different ML tasks like clustering and classification.

3.3.2. Least Absolute Shrinkage and Selection Operator (Lasso) Regression

Lasso regression is a supervised method that can be used for efficient feature selection. It is a type of regularized linear regression variants. It is a specific case of the penalized least squares regression with an L_1 penalty function. By combining the good qualities of ridge regression [45,46] and subset selection, Lasso can improve both model interpretability and prediction accuracy [47]. Lasso regression tries to minimize the following objective function:

$$\min(\text{Sum of square residuals} + \alpha \times |\text{slope}|) \quad (5)$$

where $\alpha \times |\text{slope}|$ is the penalty term. In Lasso regression, we take the absolute value of the slope in the penalty term rather than the square (as in ridge regression [46]). This helps to reduce the slope of useless variables exactly equal to zero.

3.3.3. Boruta

The last feature selection method that we are using is Boruta. It is a supervised method that is made all around the random forest (RF) classification algorithm. It works by creating shadow features so that the features do not compete among themselves but rather they compete with a randomized version of them [48]. It captures the non-linear relationships and interactions using the RF algorithm. It then extract the importance of each feature (corresponding to the class label) and only keep the features that are above a specific threshold of importance. The threshold is defined as the highest feature importance recorded among the shadow features.

3.4. Clustering Methods

In this paper, we use five different clustering methods (both hard and soft clustering approaches) namely k-means [49], k-modes [50], Fuzzy c-means [51,52], agglomerative hierarchical clustering, and Hierarchical density-based spatial clustering of applications with noise (HDBSCAN) [53,54] (note that is a soft clustering approach). For the k-means and k-modes, default parameters are used. For the fuzzy c-means, the clustering criterion used to aggregate subsets is a generalized least-squares objective function. For agglomerative hierarchical clustering, a bottom-up approach is applied, which is acknowledged as the agglomerative method. Since the bottom-up procedure starts from anywhere in the central point of the hierarchy and the lower part of the hierarchy is developed by a less expensive method such as partitional clustering, it can reduce the computational cost [55].

HDBSCAN is not just density-based spatial clustering of applications with noise (DBSCAN) but switching it into a hierarchical clustering algorithm and then obtaining a flat clustering based in the solidity of clusters. HDBSCAN is robust to parameter choice and can discover clusters of differing densities (unlike DBSCAN) [54].

3.5. Optimal number of Clusters

We determined the optimal number of clusters using the elbow method [56]. It can fit the model with number of clusters K ranging from 2 to 14. As a quality measure, 'distortion' is used, which measures the sum of squared distances from each point to its center. Figure 3 is showing the distortion score for several values of K . We also plot the training runtime (in seconds) to see the trade-off between distortion score and the runtime. We use the "knee point detection algorithm (KPDA)" [56] to determine the optimal number of clusters. Note that based on results shown in Figure 3, the perfect number of clusters is 4. However, we choose $K = 5$ for all hard clustering approaches because we have five different variants in our data (see Table 1). The KPDA chose four as the best initial number of clusters due to the Beta variant being not

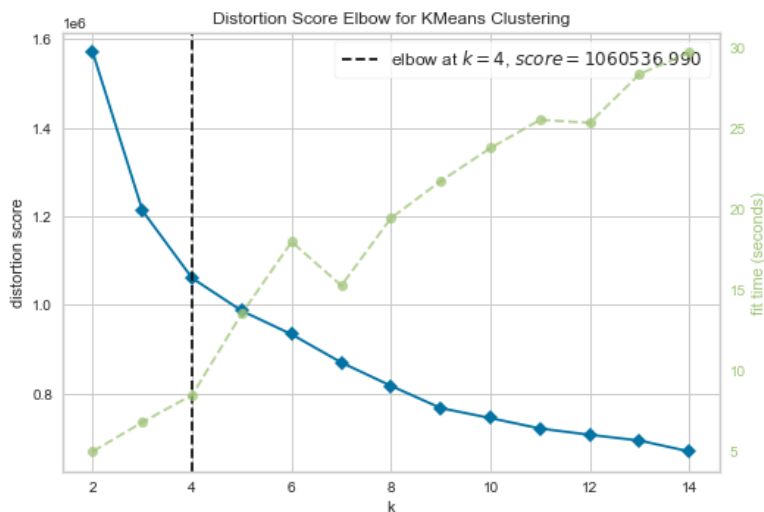


Figure 3. The distortion score (blue line) for different numbers of clusters using k -means. The dashed green line shows the runtime (in sec.). The dashed black line shows the optimal number of clusters computed using the Elbow method [56].

well-represented in the data (see Table 1). However, to give a fair chance to the Beta variant to form its own cluster, we choose 5 as the number of clusters.

4. Experimental Setup

In this section, first, we provide information associated to the dataset. Then, with the benefit of the t -distributed stochastic neighbor embedding (t -SNE) [57], we try to reduce dimensions with non-linear relationships to find any natural hidden clustering in the data. This data analysis step helps us to obtain basic knowledge about different variants. As a baseline, we use k -mers based frequency vectors without applying any feature selection to perform clustering using k -means, k -modes, fuzzy, hierarchical, and Density-based spatial (HDBSCAN) algorithms. The weighted F_1 score is used to measure the quality of clustering algorithms for different experimental settings. All experiments are performed on a Core i5 system running the Windows operating system, 32GB memory, and a 2.4 GHz processor. Implementation of the algorithms is done in Python, and the code is available online¹. Our pre-processed data is also available online², which can be used after agreeing to terms and conditions of GISAID³. The code of HDBSCAN is taken from [54]. The code for fuzzy c -means is also available online⁴.

4.1. Dataset Statistics

Our dataset is the (aligned) amino acid sequences (spike region only) of the SARS-CoV-2 proteome. The dataset is publicly available on the GISAID website⁵, which is the largest known database of SARS-CoV-2 sequences. Table 1 is showing more information related to the dataset. There are five most common variants namely Alpha, Beta, Delta, Gamma, and Epsilon. The forth column of Table 1

¹ https://github.com/sarwanpasha/COVID_19_Community_Detection_For_Variants/tree/main/Results

² <https://drive.google.com/drive/folders/1-YmIM8ipFpj-gl9hSF3t6VuofrpgWUa?usp=sharing>

³ <https://www.gisaid.org/>

⁴ <https://github.com/omadson/fuzzy-c-means>

⁵ <https://www.gisaid.org/>

shows number of mutations occurred in spike protein over the number of total mutations (in whole genome) for each variant, e.g., for Alpha variant there are 17 mutations in the whole genome and 8 of the mutations are in spike region out of those 17. In our dataset, we have 62,657 amino acid sequences (after removing missing values).

Pango Lineage	Region	Labels	Num. Mutations S-gene/Genome	Num. of sequences
B.1.1.7	UK [58]	Alpha	8/17	13966
B.1.351	South Africa [58]	Beta	9/21	1727
B.1.617.2	India [59]	Delta	8/17	7551
P.1	Brazil [60]	Gamma	10/21	26629
B.1.427	California [61]	Epsilon	3/5	12784

Table 1. Variants information and distribution in the dataset. The S/Gen. column represents number of mutations on the S gene / entire genome. Total number of amino acid sequences in our dataset is 62,657.

4.2. Data Visualization

By using the *t*-SNE approach, we plotted the data to 2D real vectors to find any hidden clustering in the data. Figure 4 (a) shows the *t*-SNE plot for the GISAID dataset (before applying any feature selection). Scattered different variants everywhere is clearly visualized. Even though we cannot see clear separate clusters for each of those variants, small clusters are obvious for different variants. This evaluation for such data reveals using any clustering algorithm directly will give us good results, and some data preprocessing is curtailed for clustering the variants efficiently.

By visualizing the GISAID dataset using *t*-SNE, more clear clusters are visible after applying three different feature selection methods. In Figure 4 (b)(c)(d), we apply different feature selection methods, namely Boruta, Lasso, and RFF, respectively. We can observe that the clustering is more pure for Boruta and Lasso regression but not for RFF. This behavior shows that the supervised methods (Lasso regression and Boruta) are able to preserve the patterns in the data more effectively as compared to the unsupervised RFF.

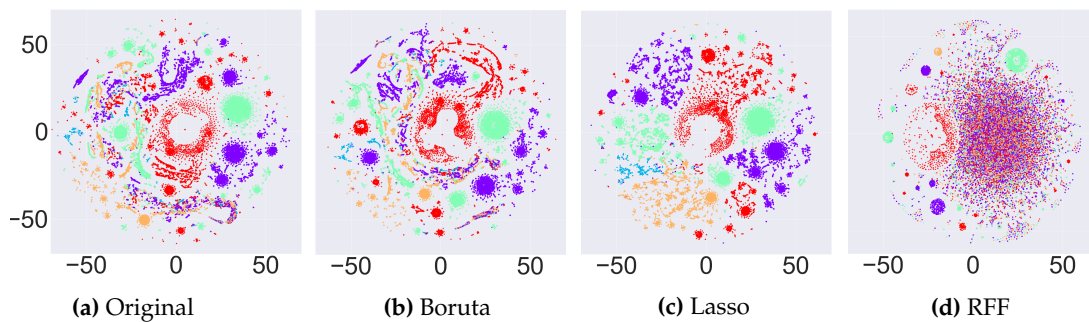


Figure 4. *t*-SNE plots for original data and for different feature selection methods applied on the original data.

5. Results and Discussion

In this section, we report the results for all clustering approaches without and with feature selection methods. We use the weighted F_1 score to compute the goodness of a clustering. Since we do not have labels available for clusters, we label each cluster using the variant that have most of its sequences in that cluster (e.g., we give the label 'Alpha' to that cluster if most of the sequences belong to the Alpha variant). Now, we calculate the F_1 score (weighted) for each cluster individually using these given labels.

For different methods, the weighted F_1 scores are provided in Table 2. Note that we did not mention the F_1 scores for HDBSCAN since it is an overlapping clustering approach. From the results, we can observe that Lasso regression is more consistent as compared to Boruta to efficiently cluster all variants. One interesting pattern we can observe is the pure clusters of some variants in case of RFF. It shows that RFF is able to cluster some variants very efficiently. However, it fails to generalize over all variants. In terms of different clustering methods, k -means and k -modes are performing better and able to generalize more on all variants as compared to the other clustering methods.

Methods	F_1 Score (Weighted) for Different Variants				
	Alpha	Beta	Delta	Gamma	Epsilon
K-means	0.359	0.157	0.611	0.690	0.443
K-means + Boruta	0.418	0.105	0.610	0.690	0.652
K-means + Lasso	0.999	0.007	0.840	0.999	0.774
K-means + RFF	1.0	0.0	0.288	1.0	1.0
K-modes	0.999	0.005	0.870	0.998	0.770
K-modes + Boruta	0.999	0.316	0.860	0.999	0.857
K-modes + Lasso	0.999	0.173	0.917	0.998	0.076
K-modes + RFF	1.0	0.0	0.0	0.613	1.0
Fuzzy	0.348	0.106	0.614	0.690	0.443
Fuzzy + Boruta	0.357	0.154	0.613	0.690	0.443
Fuzzy + Lasso	0.999	0.314	0.647	0.999	0.816
Fuzzy + RFF	0.439	0.0	0.0	1.0	0.0
Hierarchical	0.320	0.103	0.582	0.704	0.465
Hierarchical + Boruta	0.365	0.136	0.633	0.681	0.457
Hierarchical + Lasso	0.995	0.580	0.578	0.999	0.834
Hierarchical + RFF	1.0	0.0	0.288	1.0	1.0

Table 2. Variant-wise F_1 (weighted) score for different clustering methods.

5.1. Contingency Tables

After evaluating the clustering methods using weighted F_1 scores, we compute the contingency tables for variants versus clusters for different clustering approaches. The contingency tables for different clustering methods and feature selection approaches is given in Table 3 to Tables 10. In Table 3, we can observe that k -modes without applying any feature selection is outperforming k -means and also the other two clustering algorithms from Table 4. In Table 5 and Table 6, we can observe that RFF is giving pure clusters for some of the variants but performing poor on the other variants. Lasso regression in Table 7 and Table 8, we can observe that clusters started to become pure immediately when we apply lasso regression. This shows the effectiveness of this feature selection method for the clustering of spike sequences. Similarly, in Table 9 and Table 10, we can see that Boruta is not giving many pure clusters (apart from k -modes). This shows that Boruta fails to generalize over different clustering approaches and different variants.

Variant	K-means (Cluster IDs)					K-modes (Cluster IDs)				
	0	1	2	3	4	0	1	2	3	4
Alpha	1512	8762	2926	680	86	8	11492	284	330	1852
Beta	295	601	626	172	33	64	9	1604	31	19
Epsilon	956	7848	3155	638	187	0	1	8532	613	3638
Delta	2706	2605	1342	868	30	0	1	3192	3491	867
Gamma	682	22140	3016	741	50	26519	7	7	61	35

Table 3. Contingency tables of variants vs clusters (No Feature Selection).

Variant	Fuzzy (Cluster IDs)					Hierarchical (Cluster IDs)				
	0	1	2	3	4	0	1	2	3	4
Alpha	666	1515	78	2945	8762	1772	3442	650	8036	66
Beta	171	279	31	627	601	501	491	164	544	27
Epsilon	637	942	186	3172	7847	1166	3804	636	6994	184
Delta	839	2725	28	1354	2605	2997	1292	827	2411	24
Gamma	739	669	47	3034	22140	865	3501	734	21484	45

Table 4. Contingency tables of variants vs clusters (No Feature Selection).

Variant	K-means (Cluster IDs)					K-modes (Cluster IDs)				
	0	1	2	3	4	0	1	2	3	4
Alpha	0	12603	0	1363	0	12603	0	0	1363	0
Beta	0	1727	0	0	0	1727	0	0	0	0
Epsilon	0	10348	0	0	2436	10348	0	2436	0	0
Delta	0	7551	0	0	0	7551	0	0	0	0
Gamma	13076	12569	984	0	0	25632	13	0	0	984

Table 5. Contingency tables of variants vs clusters (Random Fourier Transform Feature Selection).

Variant	Fuzzy (Cluster IDs)					Hierarchical (Cluster IDs)				
	0	1	2	3	4	0	1	2	3	4
Alpha	0	0	0	13966	0	12603	0	0	1363	0
Beta	0	0	0	1727	0	1727	0	0	0	0
Epsilon	0	0	0	12784	0	10348	0	2436	0	0
Delta	0	0	0	7551	0	7551	0	0	0	0
Gamma	0	0	0	13553	13076	12569	13076	0	0	984

Table 6. Contingency tables of variants vs clusters (Random Fourier Transform Feature Selection).

Variant	K-means (Cluster IDs)					K-modes (Cluster IDs)				
	0	1	2	3	4	0	1	2	3	4
Alpha	303	11365	383	1909	6	8	10958	282	2660	58
Beta	1551	4	148	23	1	65	9	1617	12	24
Epsilon	8536	1	671	3576	0	0	1	12000	112	671
Delta	3098	0	3693	760	0	0	0	3121	19	4411
Gamma	16	13	198	36	26366	26577	7	7	0	38

Table 7. Contingency tables of variants vs clusters (Lasso Feature Selection).

Variant	Fuzzy (Cluster IDs)					Hierarchical (Cluster IDs)				
	0	1	2	3	4	0	1	2	3	4
Alpha	1344	5	12042	362	213	1967	606	30	11345	18
Beta	99	1	6	440	1181	24	1667	6	22	8
Epsilon	3220	0	0	780	8784	3667	509	8582	26	0
Delta	4464	0	0	543	2544	3892	245	3367	40	7
Gamma	202	26169	16	232	10	12	1053	1	11	25552

Table 8. Contingency tables of variants vs clusters (Lasso Feature Selection).

5.2. HDBSCAN Clustering

After doing analysis on hard clustering algorithms, we evaluate the performance of the soft clustering approach (HDBSCAN) in this section. To evaluate HDBSCAN, we use the *t*-SNE approach to plot the original variants from our data and compared them with clusters we obtained after applying HDBSCAN.

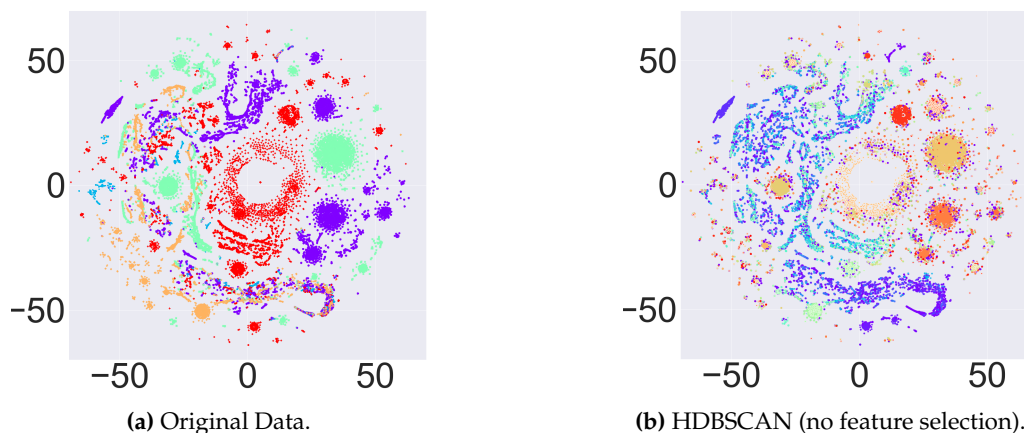
Variant	K-means(Cluster IDs)					K-modes(Cluster IDs)				
	0	1	2	3	4	0	1	2	3	4
Alpha	8762	86	2925	680	1513	11403	7	184	1823	549
Beta	601	33	626	172	295	6	6	640	1060	15
Epsilon	7848	187	3155	638	956	1	0	11170	947	666
Delta	2605	30	1342	868	2706	0	0	2894	690	3967
Gamma	22140	50	3016	741	682	6	25428	6	1128	61

Table 9. Contingency tables of variants vs clusters (Boruta Feature Selection).

Variant	Fuzzy (Cluster IDs)					Hierarchical (Cluster IDs)				
	0	1	2	3	4	0	1	2	3	4
Alpha	668	1513	78	2945	8762	9373	702	2641	1198	52
Beta	171	297	31	627	601	823	170	457	254	23
Epsilon	637	943	186	3170	7848	8419	644	2949	591	181
Delta	851	2713	28	1354	2605	2847	879	1563	2245	17
Gamma	739	669	47	3034	22140	22955	743	2330	560	41

Table 10. Contingency tables of variants vs clusters (Boruta Feature Selection).

Since this is a soft clustering approach (overlapping allowed), there were large number of clusters inferred for different feature selection methods. Therefore we use t -SNE to plot the clusters to visually observe the patterns before and after clustering. Figure 5 shows the comparison on t -SNE plot on original data versus t -SNE plots for the clustering results after applying HDBSCAN. Since overlapping is allowed in this setting, we cannot see any pure clusters as compared to the original t -SNE plot. An interesting finding from such result is that not all sequences corresponding to a specific variant are similar to each other. This means that a small cluster of sequences, that initially belong to a certain variant can make another subgroup, which could eventually lead to developing a new variant. Therefore, using such overlapping clustering approach, we can visually observe if a group of sequences are diverging from its parent variant. Biologists and other decision making authorities can then take relevant measure to deal with such scenarios. The t -SNE plots for different feature selection methods in given in Figure 6.

**Figure 5.** (a) t -SNE plots for the original variants as labels, (b) t -SNE plot with labels got after applying HDBSCAN without any feature selection method on the frequency vectors.

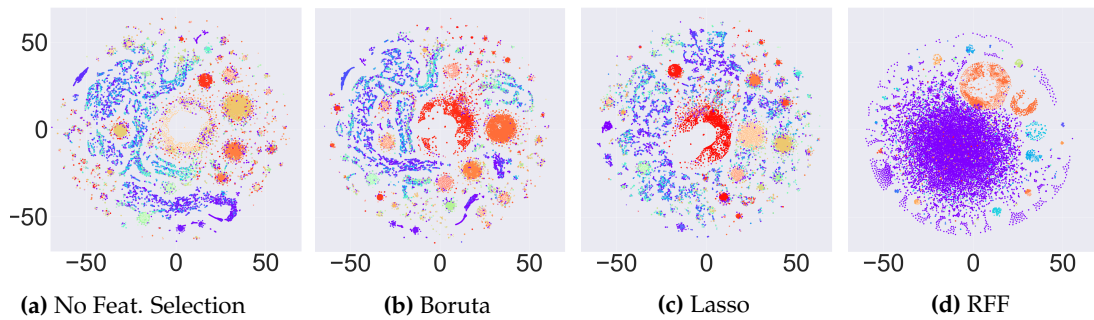


Figure 6. t-SNE plots for HDBSCAN without and with feature selection methods.

5.3. Runtime Comparison

After applying different clustering methods and feature selection algorithms on the spike sequences, we observe that k -means and k -modes are performing better than the other clustering methods in terms of weighted F_1 score. However, it is also important to study the effect of runtime for these clustering approaches so that we can evaluate the trade-off between F_1 score and the runtime. For this purpose, we compute the runtime of different clustering algorithms without and with feature selection methods. Figure 7 shows the runtime for all five clustering methods without applying any feature selection on the data. We can observe that k -modes is very expensive in terms of runtime and k -means takes the least amount of time to execute. Similar behavior is observed in Figure 8, Figure 9, and Figure 10 for RFF, Boruta, and Lasso regression, respectively. This behavior shows that although k -modes is performing better in terms of F_1 score, it is an outlier in terms of runtime. This behavior also shows the effectiveness of the k -means algorithm in terms of F_1 score and also in terms of runtime.

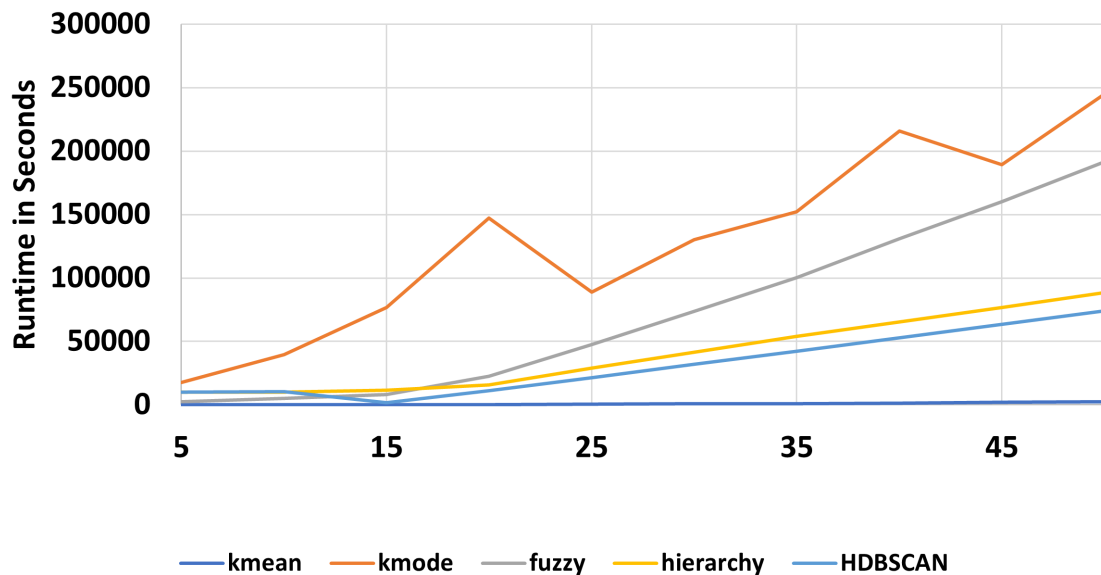


Figure 7. Running time for different clustering methods (No feature selection method). X-axis shows number of clusters.

6. Conclusion

We propose a feature vector representation and a set of feature selection methods to eliminate the less important features, allowing many different clustering methods to successfully cluster SARS-CoV-2 spike

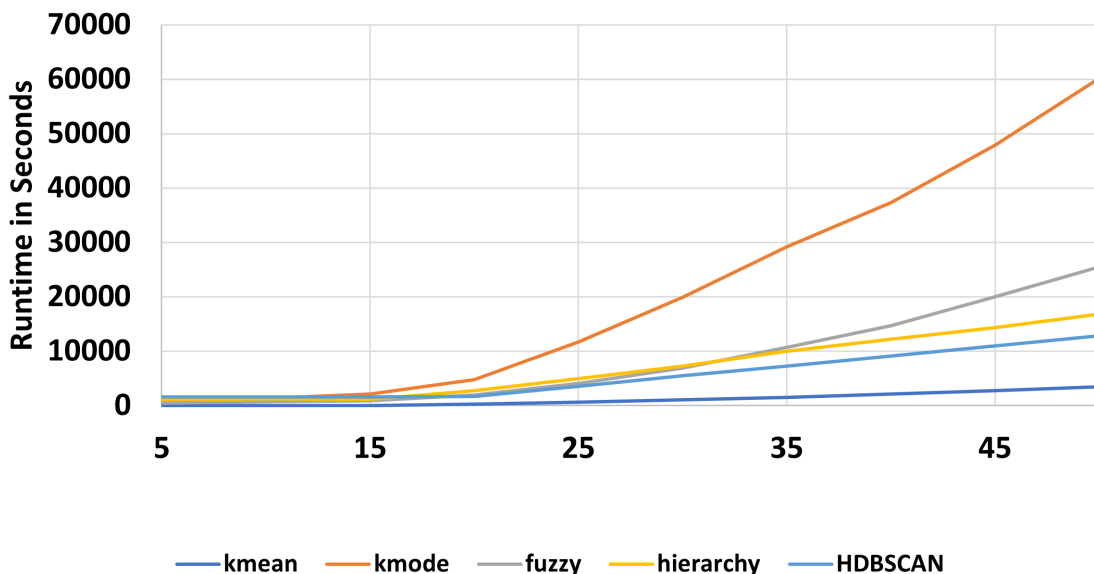


Figure 8. Running time for different clustering methods (Random Fourier Transform Feature Selection). X-axis shows number of clusters.

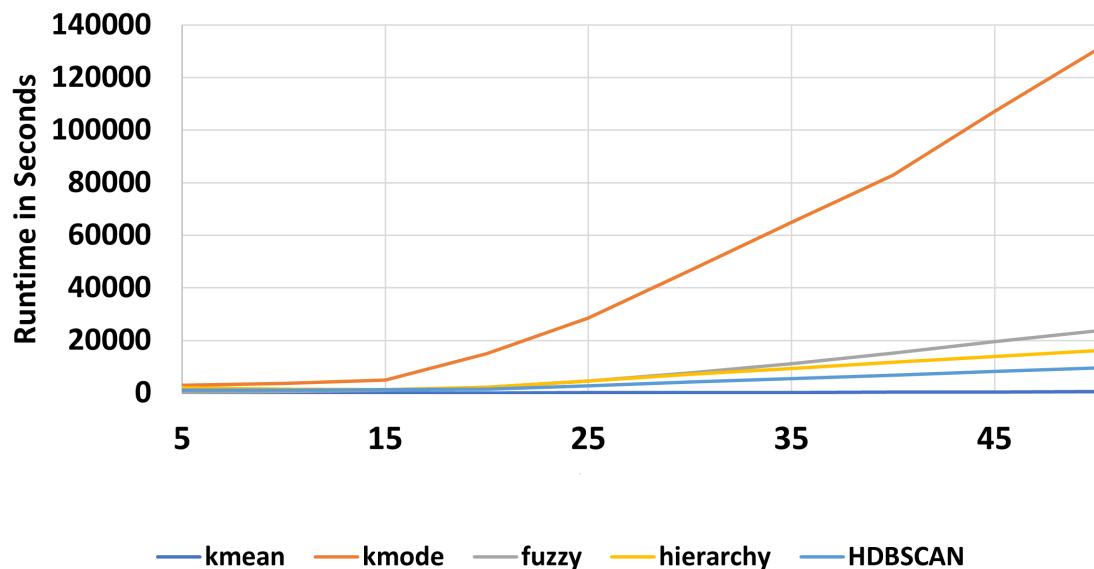


Figure 9. Running time for different clustering methods (Boruta Feature Selection). X-axis shows number of clusters.

protein sequences with high F_1 scores. We show that runtime is also an important factor while clustering the coronavirus spike sequences. The k -means algorithm is able to generalize over all variants in terms of doing pure clustering and also consuming the least amount of runtime. One possible future work is to use more data for the analysis. Testing out additional clustering methods could be another direction. Using deep learning on even bigger data could give us some interesting insights. Another interesting extension is to compute other feature vector representations, *e.g.*, based on minimizers, which can be done without the need for aligning the sequences. This would allow us to use all of this clustering machinery to study unaligned (even unassembled) sequencing reads of intra-host viral populations, to unveil the interesting dynamics at this scale.

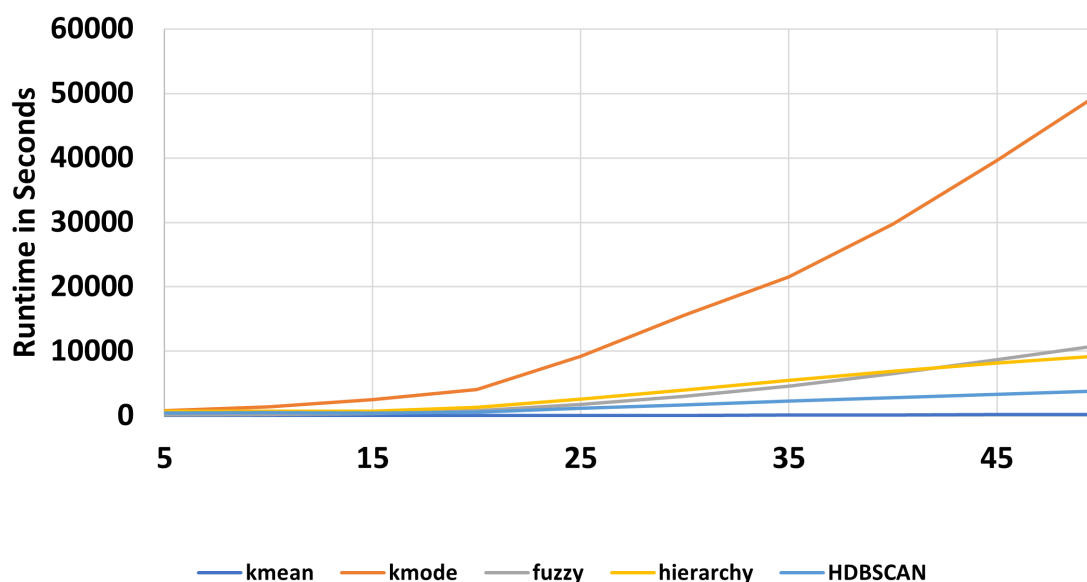


Figure 10. Running time for different clustering methods (Lasso Feature Selection). X-axis shows number of clusters.

References

1. World Health Organization. Genomic sequencing of SARS-CoV-2: a guide to implementation for maximum impact on public health, 8 January 2021. . **2021**.
2. Lu, R.; Zhao, X.; Li, J.; Niu, P.; Yang, B.; Wu, H.; Wang, W.; Song, H.; Huang, B.; Zhu, N.; others. Genomic characterisation and epidemiology of 2019 novel coronavirus: implications for virus origins and receptor binding. *The lancet* **2020**, *395*, 565–574.
3. Chen, L.; Liu, W.; Zhang, Q.; Xu, K.; Ye, G.; Wu, W.; Sun, Z.; Liu, F.; Wu, K.; Zhong, B.; others. RNA based mNGS approach identifies a novel human coronavirus from two individual pneumonia cases in 2019 Wuhan outbreak. *Emerging microbes & infections* **2020**, *9*, 313–319.
4. Chan, J.F.W.; Kok, K.H.; Zhu, Z.; Chu, H.; To, K.K.W.; Yuan, S.; Yuen, K.Y. Genomic characterization of the 2019 novel human-pathogenic coronavirus isolated from a patient with atypical pneumonia after visiting Wuhan. *Emerging microbes & infections* **2020**, *9*, 221–236.
5. Weissenhorn, W.; Dessen, A.; Calder, L.; Harrison, S.; Skehel, J.; Wiley, D. Structural basis for membrane fusion by enveloped viruses. *Molecular membrane biology* **1999**, *16*, 3–9.
6. Walls, A.C.; Park, Y.J.; Tortorici, M.A.; Wall, A.; McGuire, A.T.; Velesler, D. Structure, function, and antigenicity of the SARS-CoV-2 spike glycoprotein. *Cell* **2020**, *181*, 281–292.
7. Lan, J.; Ge, J.; Yu, J.; Shan, S.; Zhou, H.; Fan, S.; Zhang, Q.; Shi, X.; Wang, Q.; Zhang, L.; others. Structure of the SARS-CoV-2 spike receptor-binding domain bound to the ACE2 receptor. *Nature* **2020**, *581*, 215–220.
8. Gui, M.; Song, W.; Zhou, H.; Xu, J.; Chen, S.; Xiang, Y.; Wang, X. Cryo-electron microscopy structures of the SARS-CoV spike glycoprotein reveal a prerequisite conformational state for receptor binding. *Cell research* **2017**, *27*, 119–129.
9. Huang, Y.; Yang, C.; Xu, X.f.; Xu, W.; Liu, S.w. Structural and functional properties of SARS-CoV-2 spike protein: potential antivirus drug development for COVID-19. *Acta Pharmacologica Sinica* **2020**, *41*, 1141–1149.
10. Kuzmin, K.; Adeniyi, A.E.; DaSouza Jr, A.K.; Lim, D.; Nguyen, H.; Molina, N.R.; Xiong, L.; Weber, I.T.; Harrison, R.W. Machine learning methods accurately predict host specificity of coronaviruses based on spike sequences alone. *Biochemical and Biophysical Research Communications* **2020**, *533*, 553–558.

11. Harvey, W.T.; Carabelli, A.M.; Jackson, B.; Gupta, R.K.; Thomson, E.C.; Harrison, E.M.; Ludden, C.; Reeve, R.; Rambaut, A.; Peacock, S.J.; others. SARS-CoV-2 variants, spike mutations and immune escape. *Nature Reviews Microbiology* **2021**, *19*, 409–424.
12. Hadfield, J.; Megill, C.; Bell, S.; Huddleston, J.; Potter, B.; Callender, C.; Sagulenko, P.; Bedford, T.; Neher, R. Nextstrain: real-time tracking of pathogen evolution. *Bioinformatics* **2018**, *34*, 4121–4123.
13. Guyon, I.; Elisseeff, A. An introduction to variable and feature selection. *Journal of machine learning research* **2003**, *3*, 1157–1182.
14. Ngiam, K.Y.; Khor, W. Big data and machine learning algorithms for health-care delivery. *The Lancet Oncology* **2019**, *20*, e262–e273.
15. Van Der Maaten, L.; Postma, E.; Van den Herik, J.; others. Dimensionality reduction: a comparative. *J Mach Learn Res* **2009**, *10*, 13.
16. Ali, S.; Sahoo, B.; Ullah, N.; Zelikovskiy, A.; Patterson, M.D.; Khan, I. A k-mer Based Approach for SARS-CoV-2 Variant Identification. *To Appear at: International Symposium on Bioinformatics Research and Applications (ISBRA) 2021*.
17. Farhan, M.; Tariq, J.; Zaman, A.; Shabbir, M.; Khan, I. Efficient Approximation Algorithms for Strings Kernel Based Sequence Classification. *Advances in neural information processing systems (NeurIPS)*. ., 2017, pp. 6935–6945.
18. Krishnan, G.; Kamath, S.; Sugumaran, V. Predicting Vaccine Hesitancy and Vaccine Sentiment Using Topic Modeling and Evolutionary Optimization. *International Conference on Applications of Natural Language to Information Systems (NLDB)*, 2021, pp. 255–263.
19. Dwivedi, S.K.; Sengupta, S. Classification of HIV-1 Sequences Using Profile Hidden Markov Models. *PLoS ONE* **2012**, *7*.
20. Melnyk, A.; Mohebbi, F.; Knyazev, S.; Sahoo, B.; Hosseini, R.; Skums, P.; Zelikovsky, A.; Patterson, M. From alpha to zeta: Identifying variants and subtypes of SARS-CoV-2 via clustering. *Journal of Computational Biology* **2021**. to appear.
21. Ali, S.; Tamkanat-E-Ali, S.; Khan, M.A.; Khan, I.; Patterson, M.; others. Effective and scalable clustering of SARS-CoV-2 sequences. *To appear at: International Conference on Big Data Research (ICBDR) 2021*.
22. Ali, S.; Patterson, M. Spike2vec: An efficient and scalable embedding approach for covid-19 spike sequences. *arXiv preprint arXiv:2109.05019* **2021**.
23. Kuksa, P.; Khan, I.; Pavlovic, V. Generalized Similarity Kernels for Efficient Sequence Classification. *SIAM International Conference on Data Mining (SDM)*, 2012, pp. 873–882.
24. Hoffmann, H. Kernel PCA for novelty detection. *Pattern recognition* **2007**, *40*, 863–874.
25. Ali, S.; Shakeel, M.; Khan, I.; Faizullah, S.; Khan, M. Predicting attributes of nodes using network structure. *ACM Transactions on Intelligent Systems and Technology (TIST)* **2021**, *12*, 1–23.
26. Shakeel, M.H.; Karim, A.; Khan, I. A multi-cascaded deep model for bilingual sms classification. *International Conference on Neural Information Processing*, 2019, pp. 287–298.
27. Shakeel, M.H.; Faizullah, S.; Alghamidi, T.; Khan, I. Language independent sentiment analysis. *2019 International Conference on Advances in the Emerging Computing Technologies (AECT)*, 2020, pp. 1–5.
28. Shakeel, M.H.; Karim, A.; Khan, I. A multi-cascaded model with data augmentation for enhanced paraphrase detection in short texts. *Information Processing & Management* **2020**, *57*, 102204.
29. Leslie, C.; Eskin, E.; Weston, J.; Noble, W. Mismatch string kernels for SVM protein classification. *Advances in neural information processing systems (NeurIPS)*, 2003, pp. 1441–1448.
30. Hassan, Z.; Shabbir, M.; Khan, I.; Abbas, W. Estimating Descriptors for Large Graphs. *Advances in Knowledge Discovery and Data Mining (PAKDD)*, 2020, pp. 779–791.
31. Hassan, Z.; Khan, I.; Shabbir, M.; Abbas, W. Computing Graph Descriptors on Edge Streams. https://www.researchgate.net/publication/353671195_Computing_Graph_Descriptors_on_Edge_Streams.
32. Atzori, M.; others. Electromyography data for non-invasive naturally-controlled robotic hand prostheses. *Sci. data* **2014**, *1*, 1–13.

33. Ullah, A.; Ali, S.; Khan, I.; Khan, M.; Faizullah, S. Effect of Analysis Window and Feature Selection on Classification of Hand Movements Using EMG Signal. *SAI Intelligent Systems Conference (IntelliSys)*, 2020, pp. 400–415.
34. Ali, S.; Alvi, M.; Faizullah, S.; Khan, M.; Alshantqiti, A.; Khan, I. Detecting DDoS Attack on SDN Due to Vulnerabilities in OpenFlow. *International Conference on Advances in the Emerging Computing Technologies (AECT)*, 2020, pp. 1–6.
35. Ali, S.; Mansoor, H.; Arshad, N.; Khan, I. Short term load forecasting using smart meter data. *International Conference on Future Energy Systems (e-Energy)*, 2019, pp. 419–421.
36. Ali, S.; Mansoor, H.; Khan, I.; Arshad, N.; Khan, M.; Faizullah, S. Short-Term Load Forecasting Using AMI Data. *CoRR* **2020**, *abs/1912.12479*.
37. Ali, S. Cache Replacement Algorithm. *arXiv preprint arXiv:2107.14646* **2021**.
38. Ahmad, M.; Tariq, J.; Farhan, M.; Shabbir, M.; Khan, I. Who should receive the vaccine? *Australasian Data Mining Conference (AusDM)*, 2016, pp. 137–145.
39. Ahmad, M.; Ali, S.; Tariq, J.; Khan, I.; Shabbir, M.; Zaman, A. Combinatorial trace method for network immunization. *Information Sciences* **2020**, *519*, 215 – 228.
40. Ahmad, M.; Tariq, J.; Shabbir, M.; Khan, I. Spectral Methods for Immunization of Large Networks. *Australasian Journal of Information Systems* **2017**, *21*.
41. Tariq, J.; Ahmad, M.; Khan, I.; Shabbir, M. Scalable Approximation Algorithm for Network Immunization. *Pacific Asia Conference on Information Systems (PACIS)*, 2017, p. 200.
42. Devijver, P.; Kittler, J. *Pattern Recognition: A Statistical Approach*. London, GB: Prentice-Hall, 1982, pp. 1–448.
43. Ali, S.; Mansoor, H.; Khan, I.; Arshad, N.; Khan, M.A.; Faizullah, S. Short-term load forecasting using AMI data. *preprint, arXiv:1912.12479* **2019**.
44. Rahimi, A.; Recht, B.; others. Random Features for Large-Scale Kernel Machines. *NIPS*, 2007, p. 5.
45. Hoerl, A.E.; Kannard, R.W.; Baldwin, K.F. Ridge regression: some simulations. *Communications in Statistics-Theory and Methods* **1975**, *4*, 105–123.
46. McDonald, G.C. Ridge regression. *Wiley Interdisciplinary Reviews: Computational Statistics* **2009**, *1*, 93–100.
47. Muthukrishnan, R.; Rohini, R. LASSO: A feature selection technique in predictive modeling for machine learning. 2016 IEEE international conference on advances in computer applications (ICACA). IEEE, 2016, pp. 18–20.
48. Kurşa, M.B.; Rudnicki, W.R.; others. Feature selection with the Boruta package. *J Stat Softw* **2010**, *36*, 1–13.
49. Fahim, A.; Salem, A.; Torkey, F.A.; Ramadan, M. An efficient enhanced k-means clustering algorithm. *Journal of Zhejiang University-Science A* **2006**, *7*, 1626–1633.
50. Khan, S.S.; Ahmad, A. Cluster center initialization algorithm for K-modes clustering. *Expert Systems with Applications* **2013**, *40*, 7444–7456.
51. Bezdek, J.C.; Ehrlich, R.; Full, W. FCM: The fuzzy c-means clustering algorithm. *Computers & geosciences* **1984**, *10*, 191–203.
52. Dias, M.L.D. fuzzy-c-means: An implementation of Fuzzy C-means clustering algorithm., 2019. doi:10.5281/zenodo.3066222.
53. Campello, R.J.; Moulavi, D.; Sander, J. Density-based clustering based on hierarchical density estimates. *Pacific-Asia conference on knowledge discovery and data mining*, 2013, pp. 160–172.
54. McInnes, L.; Healy, J.; Astels, S. hdbscan: Hierarchical density based clustering. *Journal of Open Source Software* **2017**, *2*, 205.
55. Bouguettaya, A.; Yu, Q.; Liu, X.; Zhou, X.; Song, A. Efficient agglomerative hierarchical clustering. *Expert Systems with Applications* **2015**, *42*, 2785–2797.
56. Satopaa, V.; Albrecht, J.; Irwin, D.; Raghavan, B. Finding a "kneedle" in a haystack: Detecting knee points in system behavior. *International conference on distributed computing systems workshops*. IEEE, 2011, pp. 166–171.
57. Van der M., L.; Hinton, G. Visualizing data using t-SNE. *Journal of Machine Learning Research (JMLR)* **2008**, *9*.

58. Galloway, S.; others. Emergence of SARS-CoV-2 b. 1.1. 7 lineage. *Morbidity and Mortality Weekly Report* **2021**, *70*, 95.
59. Yadav, P.; others. Neutralization potential of Covishield vaccinated individuals sera against B. 1.617. 1. *bioRxiv* **2021**, *1*.
60. Naveca, F.; others. Phylogenetic relationship of SARS-CoV-2 sequences from Amazonas with emerging Brazilian variants harboring mutations E484K and N501Y in the Spike protein. *Virological.org* **2021**, *1*.
61. Zhang, W.; others. Emergence of a novel SARS-CoV-2 variant in Southern California. *Jama* **2021**, *325*, 1324–1326.

© 2021 by the authors. Submitted to *Journal Not Specified* for possible open access publication under the terms and conditions of the Creative Commons Attribution (CC BY) license (<http://creativecommons.org/licenses/by/4.0/>).